Hindawi
International Journal of Antennas and Propagation
Volume 2019, Article ID 4391474, 10 pages
https://doi.org/10.1155/2019/4391474

Research Article

Ultra-Wideband Dielectric Resonator Antenna Design Based on Multilayer Form

Fan Wang,[1] **Chuanfang Zhang**,[1] **Houjun Sun**,[1] **and Yu Xiao**[2]

[1]*School of Information and Electronics, Beijing Institute of Technology, Beijing 100081, China*
[2]*Department of Electronic Engineering, Tsinghua University, Beijing 100084, China*

Correspondence should be addressed to Chuanfang Zhang; zcf@bit.edu.cn

Received 15 January 2019; Revised 28 March 2019; Accepted 3 April 2019; Published 16 April 2019

Academic Editor: Paolo Burghignoli

In this paper, an ultra-wideband dielectric resonator antenna (DRA) is investigated. It basically covers the bandwidth from 6 GHz to 16 GHz and achieves a relative bandwidth of 90.9%. It is found that a wide bandwidth can be reached with a small DRA by adopting multilayer form. Thus, the dimension of the designed DRA element which is composed of nine-element phased-scanning linear array is as small as 6.9mm x 8.2mm x 11 mm. While the maximum stable zenith gain is 6.2dB, the lobe width is 3 dB. The operating frequency range of the antenna array is from 5.42GHz to 16.5GHz, achieving a 101.1% relative bandwidth. A large scanning angle of ±60° is realized within the operating frequency band, with good scanning pattern and cross polarization. To verify the design and simulation, a 1 × 9 DRA array is fabricated, and measurements are carried out.

1. Introduction

Ultra-wideband technology, as one of the key technologies for integrated radio frequency, plays an important role in the integrated radio frequency system. It is an important foundation for the upgrading of avionics systems. Over the past decades, the rapid development of microwave materials and electromagnetic simulation technology has laid a good foundation for the research and development of the dielectric resonator antenna (DRA). The DRA is relatively simple to fabricate and easy to excite. It has a lightweight as well as a compact structure. The main radiation structure of the DRA is composed of the microwave material with very low loss, and the antenna is radiating through the surface of the entire resonator except the ground. Since there is no metal material, no conductor and surface wave loss exist, which induces a very high radiation efficiency. The DRA has a variety of structures and large degrees of design freedom with three-dimensional structure. The basic way to extend the DRA bandwidth is to reduce the Q-factor of the antenna by lessening the permittivity of the dielectric material. This method is mainly suitable for a single mode of operation. In addition, the introduction of multimode resonance is also an important approach to extend the bandwidth of the DRA. A DRA working on a high operating bandwidth (exceeding 65% fractional bandwidth) realized with a hollow dielectric cylinder equipped with a top-mount spherical cap-lens and a suitably shaped metal reflector is presented in [1]. This antenna allows achieving a high-gain (exceeding 14 dBi), excellent linear/circular polarization purity, and a high front-to-back ratio (better than 20 dB), while a cylindrical DRA which employs some layers of uniaxial anisotropic materials to increase the directivity of the antenna in the boresight direction is proposed in [2]. A cylindrical structure DRA to expand the bandwidth is introduced in [3]. Coaxial feed and aperture coupled feed are used for exciting the antenna. The impedance bandwidth is 26.8% for coaxial feed and 23.7% for aperture coupled feed. DRAs of four different cone shape structures are designed in [4]. It can be seen that the bandwidth of the inverted cone structure is wider than that of the noninverted cone structure. Besides, the split cone structure excites more modes than all the other cone structures and has a much wider bandwidth that almost reached 50%. A dielectric material ($\varepsilon_r = 20$) is used as the radiation body to design a DRA with the conical structure in [5]. This antenna is fed through the micro-strip line,

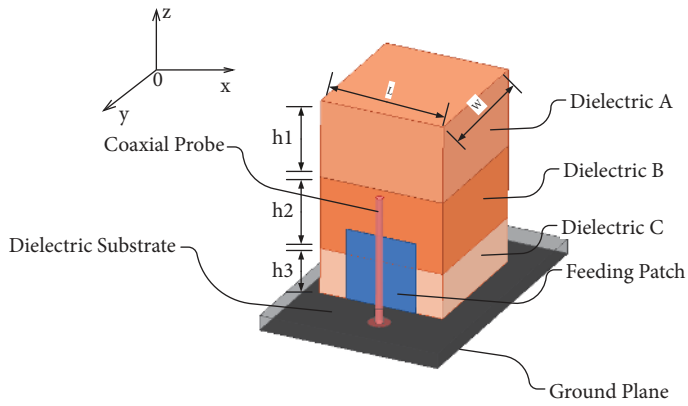

Figure 1: Configuration of the DRA element.

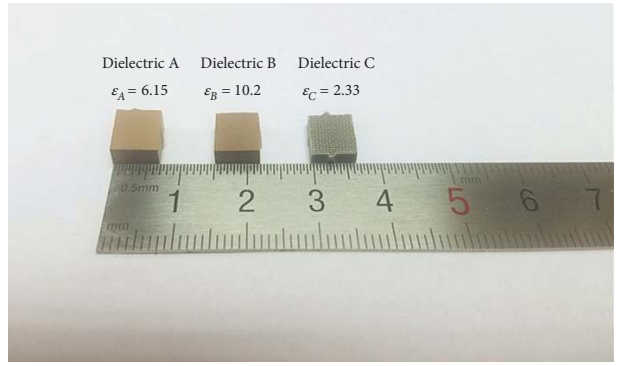

Figure 2: Prototype of three dielectric materials.

which simultaneously excites the fundamental mode and the higher order mode and finally achieves a bandwidth of 2.72-11.36 GHz. Multilayer dielectric structure is used in [6–9]. It is also an effective way to extend the bandwidth of DRA. An X-band wideband stair-shaped structure DRA is introduced in [10]. By using the two-step stair-shaped structure, the DRA obtains an impedance bandwidth ($S_{11} < -10dB$) of 54.3%. Another effective way to extend the bandwidth is making use of hybrid radiating structure, as shown in [11].

The phased array DRA with characteristics of miniaturization and ultra-wideband is designed and discussed in the paper. The DRA element is composed of nine-element phased-scanning linear array and is expanded in a multilayer form. The return loss is reduced by adding a metal patch. This DRA can be used for the terminal equipment of satellite communication system (8/7GHz X-band and 14/11GHz Ku-band) as well as the weather radar system.

2. DRA Element Design

Ultra-wideband is one of the important trends in the development of DRA. For a single dielectric material DRA, high-permittivity is required to reduce the size of the antenna. However, using high-permittivity dielectric material is equivalent to improving the Q-factor of the dielectric resonator which reduces the antenna operating bandwidth. That is, miniaturization and ultra-wideband for a single dielectric material DRA are contradictory. Thus an additional approach needs to be considered to overcome the problem. To expand the bandwidth of DRA, using the multilayer forms such as laminates composed of dielectrics with same cross-sectional dimension and different permittivities, or structures introducing suitable air layers ($\varepsilon_r = 1$) is an effective way. Due to different natural resonant frequencies of the dielectric materials, multimode resonances will be generated and the bandwidth will be expanded.

Compared with other geometric forms of DRA, the rectangular form DRA has the advantages of being fabricated simply and possessing high design freedom. Thus, the proposed antenna element is designed in this form. According to [12], the resonant frequency of the fundamental mode of the rectangular formed DRA can be approximately computed as

$$f_0 = \frac{15\left[a_1 + a_2\,(w/2h) + 0.16\,(w/2h)^2\right]}{w\pi\sqrt{\varepsilon_r}} \quad (1)$$

$$a_1 = 2.57 - 0.8\left(\frac{d}{2h}\right) + 0.42\left(\frac{d}{2h}\right)^2 - 0.05\left(\frac{d}{2h}\right)^3 \quad (2)$$

$$a_2 = 2.71\left(\frac{d}{2h}\right)^{-0.282} \quad (3)$$

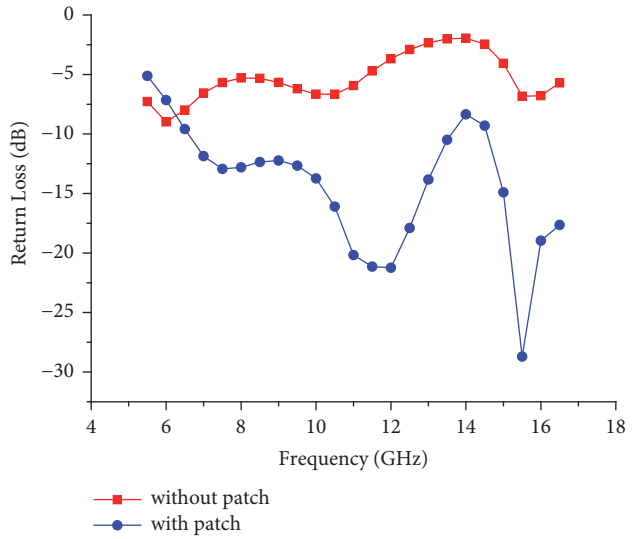

Figure 3: Return loss comparison (with and without metal patch) of the DRA element.

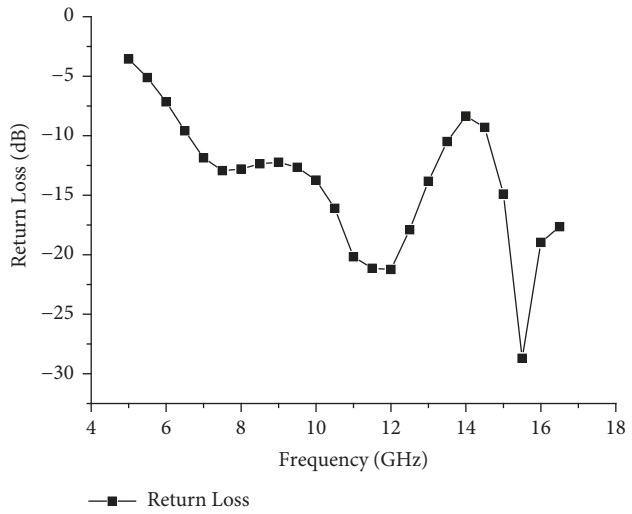

Figure 4: Return loss of the DRA element.

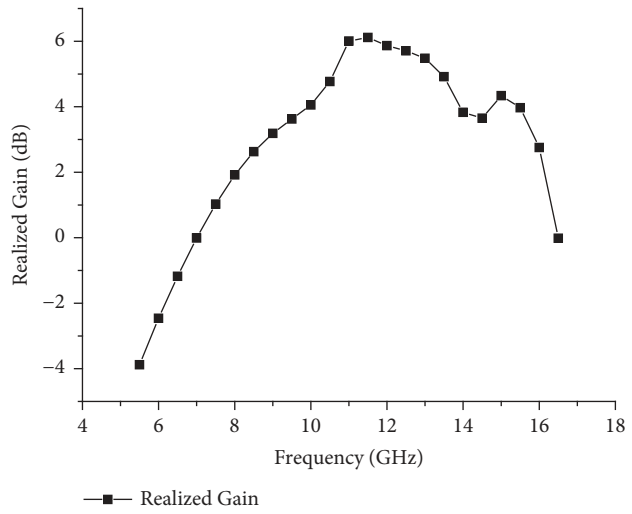

Figure 5: Realized gain of the DRA element.

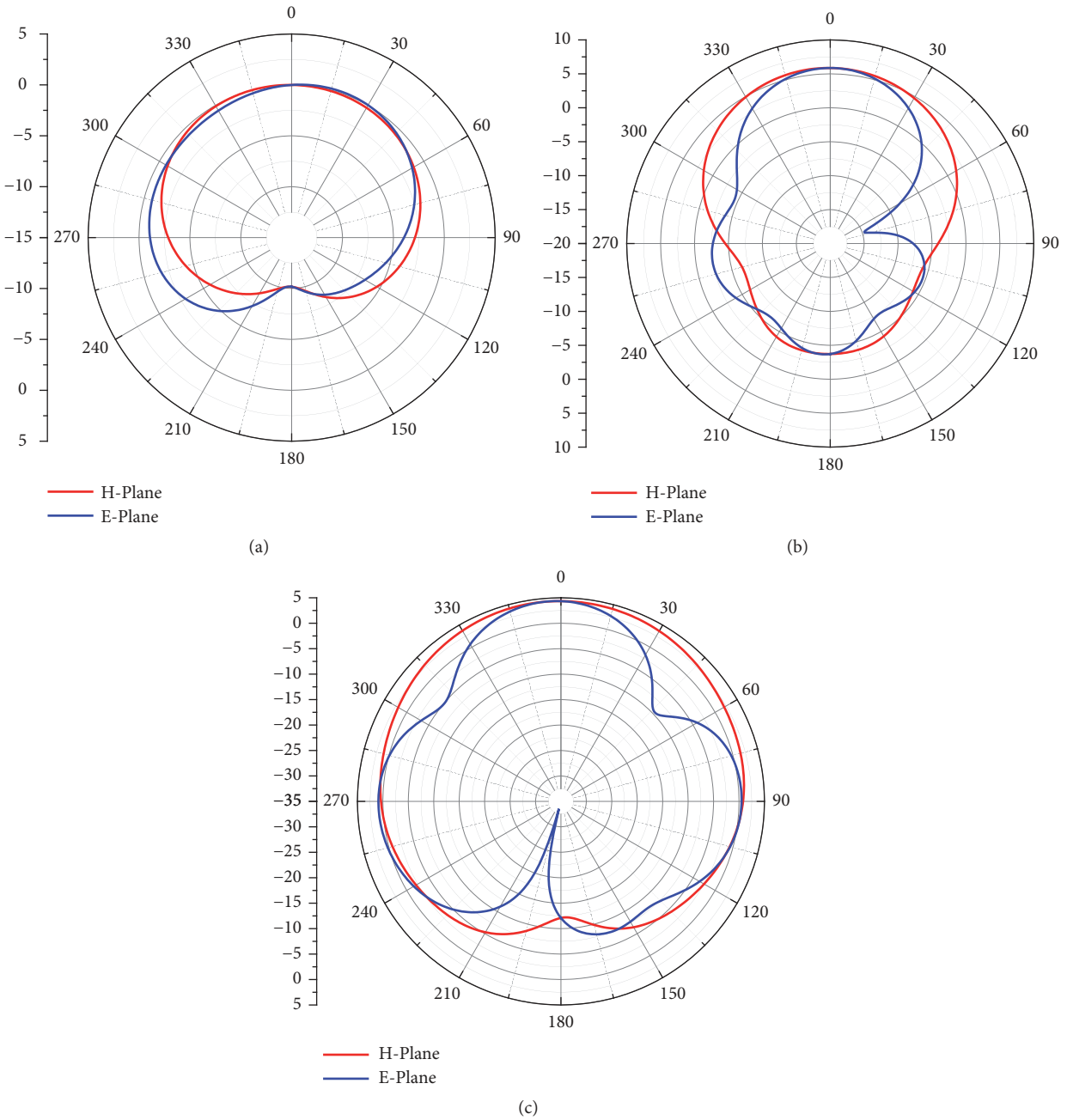

Figure 6: E-plane and H-plane radiation patterns of the DRA element (a) at 7 GHz, (b) at 12 GHz, and (c) at 15 GHz.

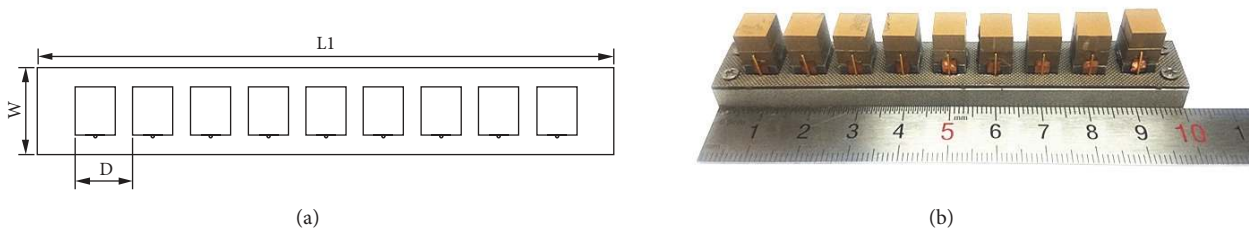

Figure 7: Configuration of the DRA array. (a) Array elements arrangement diagram. (b) Prototype of the proposed DRA array.

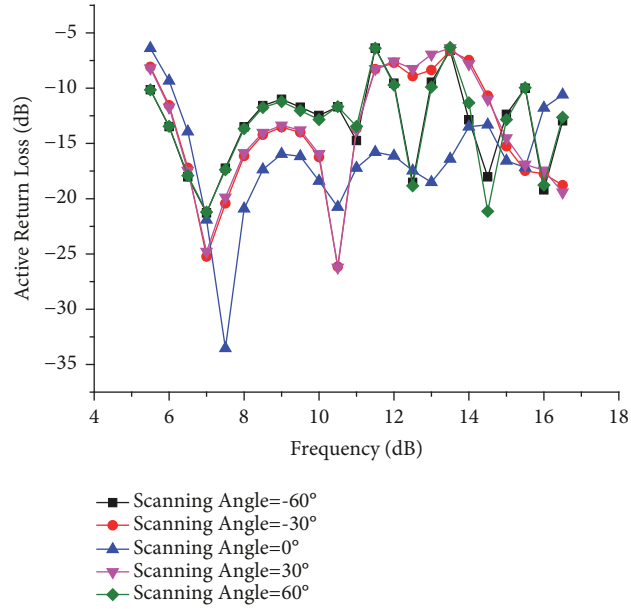

Figure 8: Active return loss of the DRA array.

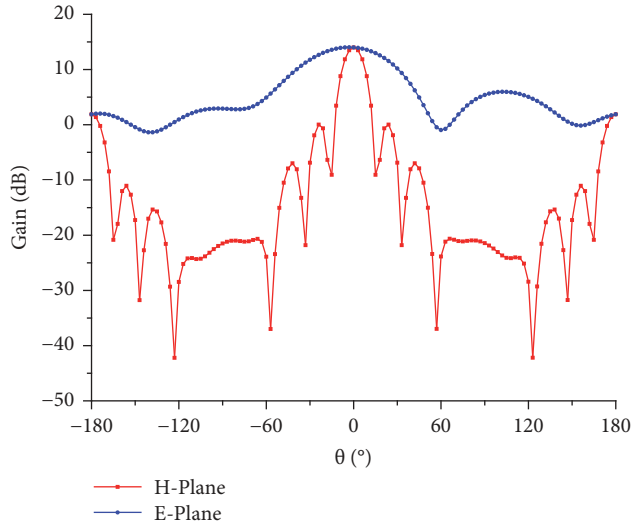

Figure 9: E-plane and H-plane radiation patterns of the DRA array at 12 GHz.

where d, w, h are the length, width, and height of the rectangular resonator, respectively.

Considering the availability and resonance characteristics of the dielectric, three different dielectrics are chosen for DRA design. The initial dimensions of the antenna are designed by (1), (2), and (3), and the antenna dimensions and dielectric arrangement are optimized by simulation software. Figure 1 depicts the configuration of the optimized DRA element. As shown in Figure 1, the antenna consists of three dielectrics: dielectric A, dielectric B, and dielectric C. They have the same cross-sectional dimensions and different permittivities. The dimensions are $L = 8.2mm$, $W = 6.9mm$, $h1 = 4.3mm$, $h2 = 4mm$, and $h3 = 2.5mm$, respectively. The permittivities are $\varepsilon_A = 6.15$, $\varepsilon_B = 10.2$, and $\varepsilon_C = 2.33$, respectively, as shown in Figure 2. The thickness of dielectric substrate is 0.813mm, and the permittivity is $\varepsilon_S = 3.55$. The connector used to excite the antenna is the SMP connector, and the length and diameter of the electrical probe are 7 mm and 0.4mm, respectively. The diameter of the hole in the ground plane which the probe passes through is 0.5mm. The length and width of the ground plane are 15 mm and 10 mm, respectively. A copper piece (length and width are 3.9mm) with a thickness of 0.03 mm is added between the side of the antenna and the coaxial probe as the feeding patch to improve the impedance matching between them and thereby optimizing the return loss. The commercial product used to glue the three layers

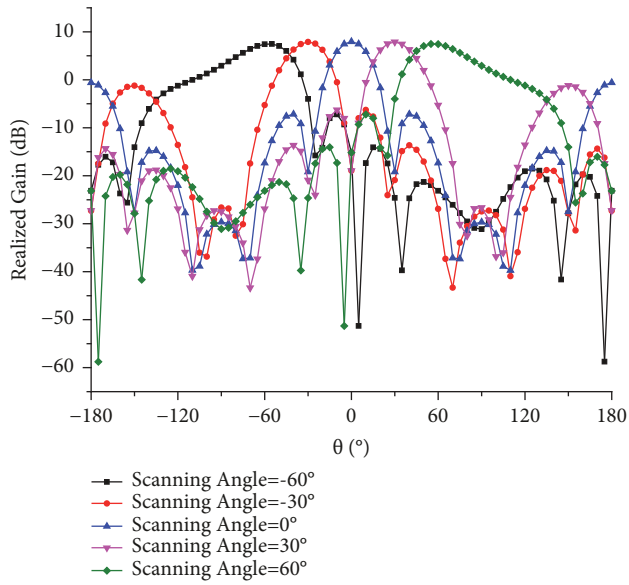

Figure 10: H-plane radiation patterns at $\theta = 0^{\circ}, \pm 30^{\circ}, \pm 60^{\circ}$ of the DRA array at 7 GHz.

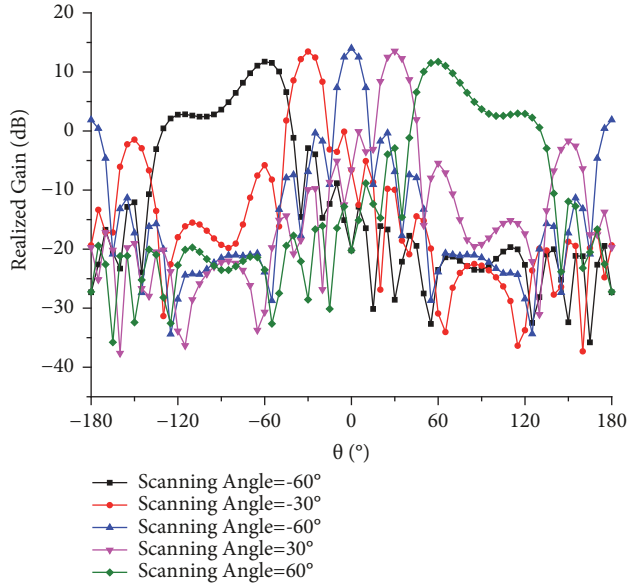

Figure 11: H-plane radiation patterns at $\theta = 0^{\circ}, \pm 30^{\circ}, \pm 60^{\circ}$ of the DRA array at 12 GHz.

is All Purpose AA Extra-glue produced by ARON ALPHA. The effect of the metal patch on the return loss of the DRA is shown in Figure 3.

The DRA element is analyzed and optimized by using the electromagnetic simulation software HFSS. Figure 4 shows the simulated return loss of the DRA. It is shown that the return loss is better than -8dB when the frequency ranges from 6 GHz to 16 GHz. Figure 5 depicts the change of simulated realized gain of the DRA with frequency variation. It is clear that the zenith gain of the antenna keeps increasing to the peak of 6.21dB at 11.2 GHz and then gradually decreases due to the slight cracking of the antenna beam at high frequencies.

Figure 6 illustrates the E-plane (YOZ-plane) and H-plane (XOZ-plane) radiation patterns of the DRA element at 7 GHz, 12 GHz, and 15 GHz, respectively. From these graphs, several conclusions can be drawn: (a) the antenna has a good directional radiation characteristic at 7 GHz, where the 3 dB lobe width is widely reaching $\pm 91^{\circ}$ and the zenith gain is 0 dB; (b) the antenna also shows a good directional radiation characteristic at 12 GHz, where the 3 dB lobe width reaches $\pm 60^{\circ}$ with the zenith gain being 5.86dB; (c) the zenith gain drops to 4.33dB at 15 GHz, and the antenna exhibits a slight beam cracking due to the exciting of high-order mode; (d) the front-to-back ratio of the DRA element is better than 9.6dB.

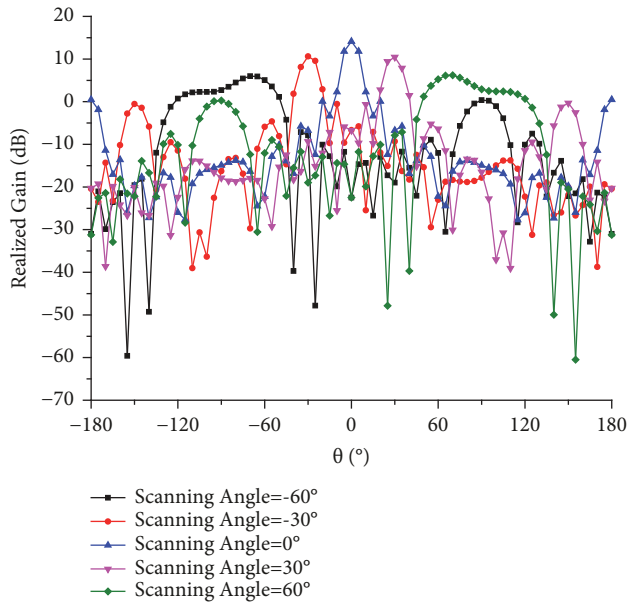

Figure 12: H-plane radiation patterns at $\theta = 0^{\circ}, \pm 30^{\circ}, \pm 60^{\circ}$ of the DRA array at 15 GHz.

Table 1: Main technical specification of the DRA array.

Technical indicator	Requirement
Operating frequency band	$6GHz$ *to* $16GHz$
Active standing wave ratio	$\rho < 3$
Scan angle	$\theta > 60^{\circ}$@$6GHz$ *to* $12GHz$
	$\theta > 30^{\circ}$@$12GHz$ *to* $16GHz$

3. DRA Array Design

The proposed DRA element is extended to a linear array with 1×9 elements. The main technical requirements of the DRA array are shown in Table 1.

In order to avoid the grating lobes of the antenna array during scanning, the element spacing d needs to follow

$$d \leq \frac{(1 - 1/N)\,\lambda}{1 + |\sin \theta_S|} \tag{4}$$

where λ is the free-space wavelength corresponding to the highest operation frequency of the antenna array; θ_S is the maximum scan angle of the antenna array; N is the number of the elements.

According to (4) and Table 1, it can be obtained that $d \leq 12.5mm$.

Figure 7 shows the configuration of the DRA array. Nine DRA elements are placed on the dielectric substrate at equal intervals along the H-plane. The dimensions of the array are $L1 = 100mm$, $W = 15mm$, and $D = 10mm$, respectively.

Figure 8 depicts the active return loss of the DRA array at the scan angles of $\theta = 0^{\circ}, \pm 30^{\circ}, \pm 60^{\circ}$. It can be seen that all active return losses are better than -6dB. The E-plane and H-plane radiation patterns at 12 GHz without scanning are shown in Figure 9. The maximum gain of the DRA array exceeds 14 dB. When the operating frequencies are 7 GHz, 12 GHz, and 15 GHz, the H-plane radiation patterns of the DRA array at different scan angles are given from Figures 10–12. Taking the case when the scan angle is 60°, the array gains are 7.49dB, 11.77dB, and 6.25dB when the operating frequencies are 7 GHz, 12 GHz, and 15 GHz, respectively.

The primary polarization and cross polarization of the DRA array are shown in Figure 13.The E-plane cross-polarization level of the DRA array is less than -29.6dB and the H-plane cross-polarization level is less than -15.6dB in all cases.

4. Experiments and Discussions

To verify the feasibility of the design, a DRA array is fabricated and measured in microwave anechoic chamber. Due to the limitations of the test conditions, the characteristics of the element in the array are mainly measured. The comparisons between the measurement results and the simulation results are shown in Figures 14 and 15.

Figure 14 shows the comparison of the return loss between measurement and simulation. As seen clearly in the graph, actual measured result of the antenna return loss is basically better than 10 dB when the frequency ranges from 6 GHz to 16 GHz. However, there is a slight difference from the simulation result that the resonance point of the measured result is slightly increased. The main reason for this result is that the air gap is introduced when the uneven application of the glue occurs during fabricating the dielectric block, which causes multiple resonances of the antenna. Figure 15 depicts the comparison of radiation patterns between measurement and simulation. The measured radiation patterns of the antenna have some differences from the simulation results mainly because of the fabricating tolerances of the antenna and the permittivity deviations of the dielectric plate. Moreover, measurement errors and effect

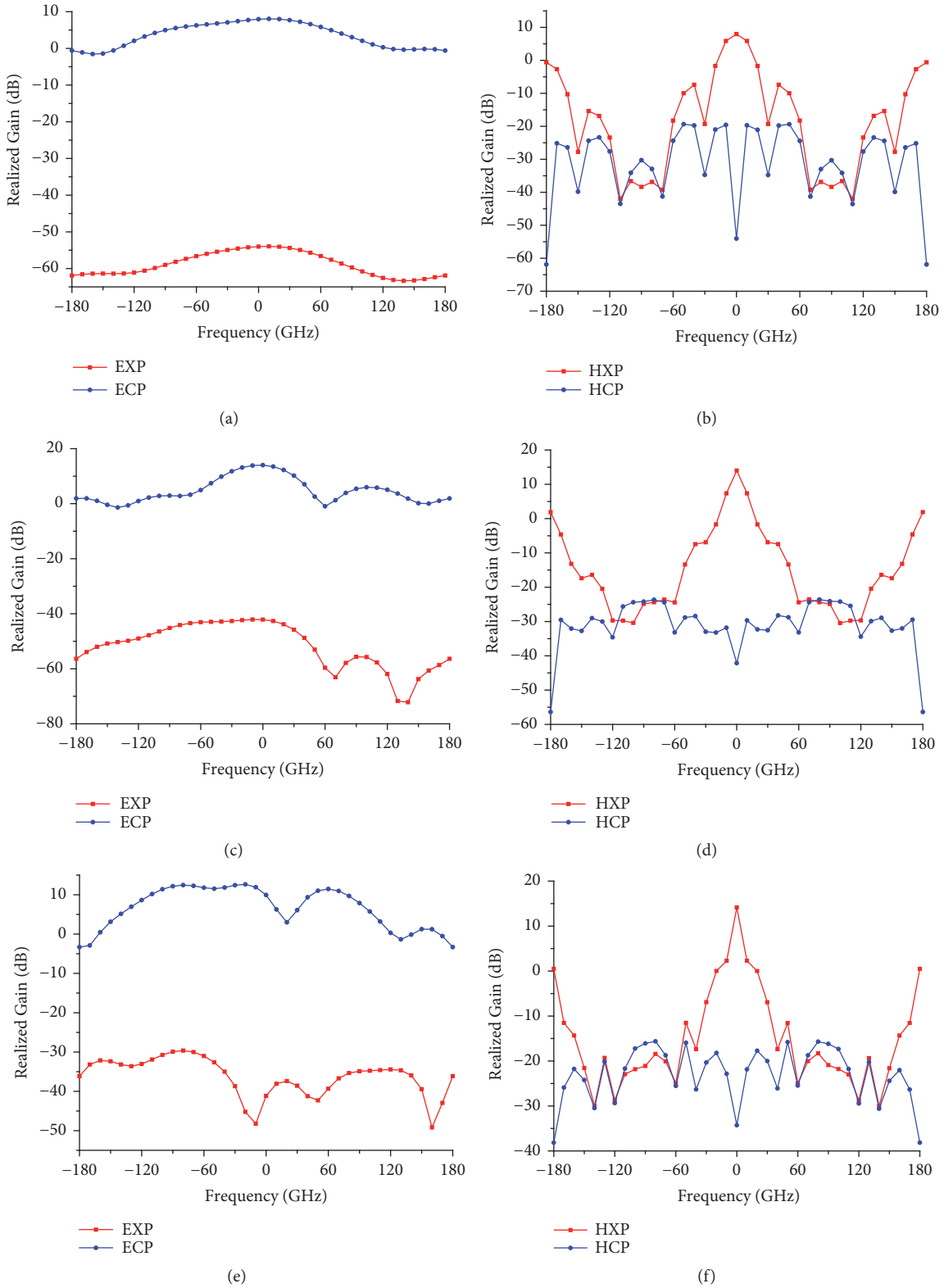

Figure 13: Primary polarization and cross polarization of the DRA array. (a) E-plane at 7 GHz. (b) H-plane at 7 GHz. (c) E-plane at 12 GHz. (d) H-plane at 12 GHz. (e) E-plane at 15 GHz. (f) H-plane at 15 GHz.

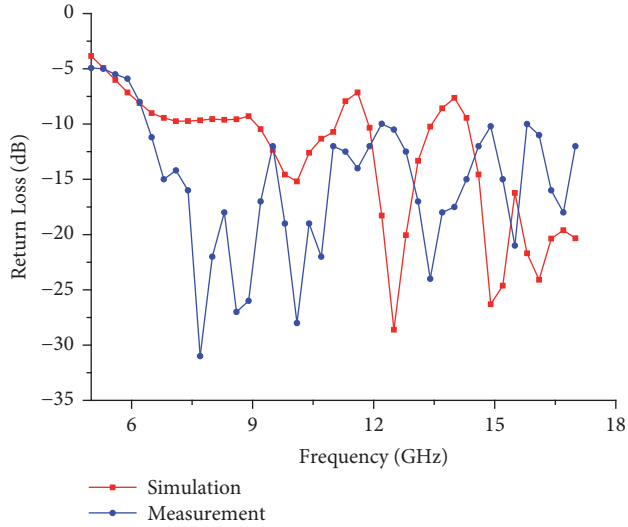

Figure 14: Comparison of return loss between measurement and simulation.

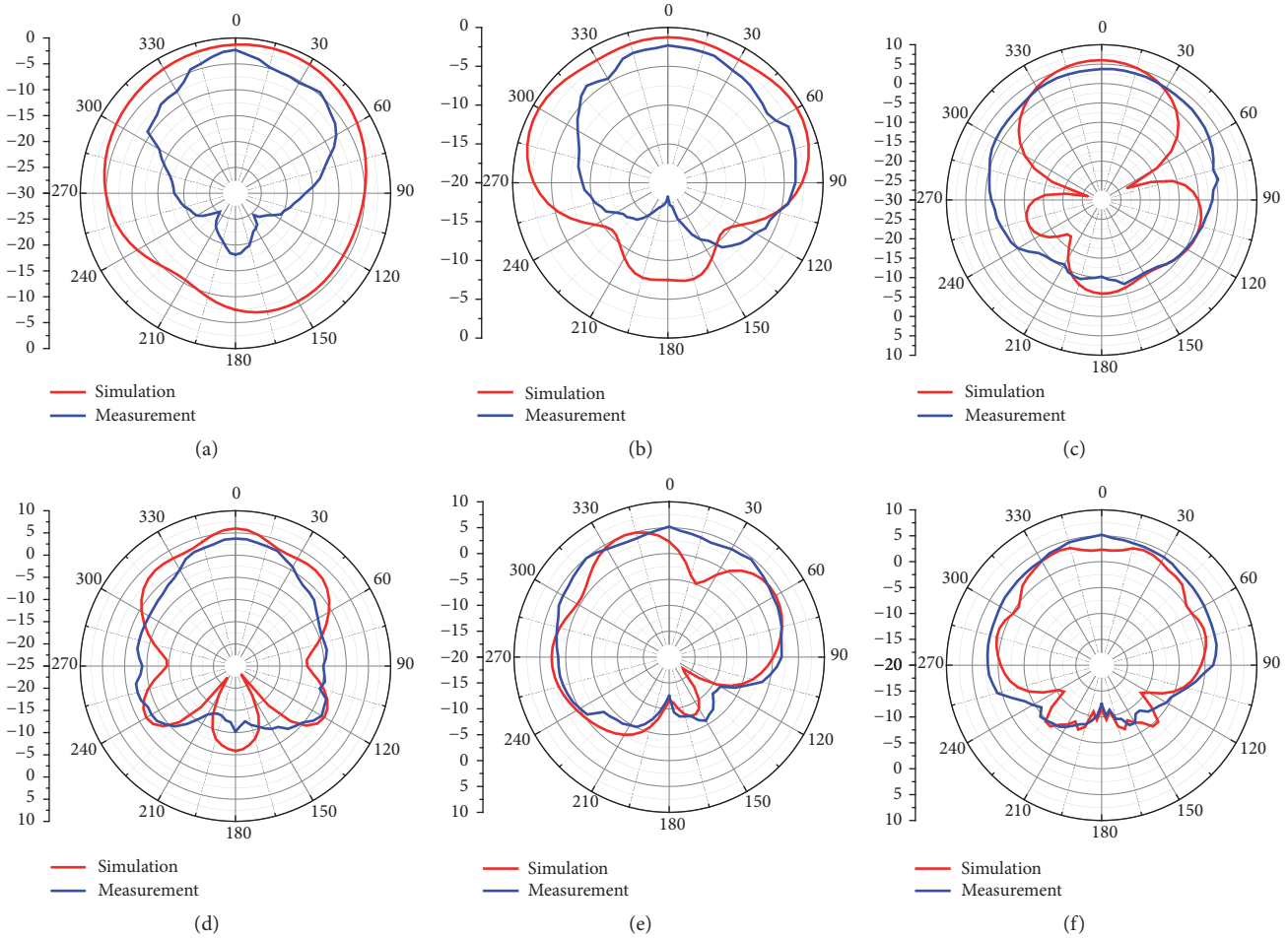

Figure 15: Comparison of radiation patterns between measurement and simulation. (a) E-plane at 6 GHz. (b) H-plane at 6 GHz. (c) E-plane at 11 GHz. (d) H-plane at 11 GHz. (e) E-plane at 16 GHz. (f) H-plane at 16 GHz.

of the SMP connector also lead the discrepancy between the simulation and measurement results. Such discrepancies are also observed in [2, 13, 14].

5. Conclusions

When studying an ultra-wideband DRA covering the bandwidth from 6 GHz to 16 GHz, it is found that the DRA element can achieve a relative bandwidth of 90.9% by adopting multilayer form. The designed DRA element composed of a nine-element phased-scanning linear array can finally achieve a 101.1% relative bandwidth. By both simulating with ANSYS HFSS and carrying out experiments, the correctness of the simulation is verified and the actual performance is acceptable.

Data Availability

The data used to support the findings of this study are included within the article.

Conflicts of Interest

The authors declare that there are no conflicts of interest regarding the publication of this paper.

References

[1] R. Cicchetti, A. Faraone, E. Miozzi, R. Ravanelli, and O. Testa, "A high-gain mushroom-shaped dielectric resonator antenna for wideband wireless applications," *IEEE Transactions on Antennas and Propagation*, vol. 64, no. 7, pp. 2848–2861, 2016.

[2] S. Fakhte, H. Oraizi, L. Matekovits, and G. Dassano, "Cylindrical anisotropic dielectric resonator antenna with improved gain," *Institute of Electrical and Electronics Engineers. Transactions on Antennas and Propagation*, vol. 65, no. 3, pp. 1404–1409, 2017.

[3] R. Chair, A. A. Kishk, and K. F. Lee, "Wideband simple cylindrical dielectric resonator antennas," *IEEE Microwave and Wireless Components Letters*, vol. 15, no. 4, pp. 241–243, 2005.

[4] A. A. Kishk, Y. Yin, and A. W. Glisson, "Conical dielectric resonator antennas for wide-band applications," *IEEE Transactions on Antennas and Propagation*, vol. 50, no. 4, pp. 469–474, 2002.

[5] G. Varshney, P. Praveen, R. S. Yaduvanshi, and V. S. Pandey, "Conical shape dielectric resonator antenna for ultra wide band applications," in *Proceedings of the 2015 International Conference on Computing, Communication and Automation, ICCCA 2015*, pp. 1304–1307, India, May 2015.

[6] Y. Ge, K. P. Esselle, and T. S. Bird, "Compact dielectric resonator antennas with ultrawide 60%–110% bandwidth," *IEEE Transactions on Antennas and Propagation*, vol. 59, no. 9, pp. 3445–3448, 2011.

[7] G. D. Makwana and D. Ghodgaonkar, "Wideband stacked rectangular dielectric resonator antenna at 5.2 GHz," *International Journal of Electromagnetics and Applications*, vol. 2, no. 3, pp. 41–45, 2012.

[8] W. Huang and A. A. Kishk, "Compact wideband multi-layer cylindrical dielectric resonator antennas," *IET Microwaves, Antennas & Propagation*, vol. 1, no. 5, pp. 998–1005, 2007.

[9] Y. M. Pan and S. Y. Zheng, "A low-profile stacked dielectric resonator antenna with high-gain and wide bandwidth," *IEEE Antennas and Wireless Propagation Letters*, vol. 15, pp. 68–71, 2016.

[10] R. Chair, A. A. Kishk, and K. F. Lee, "Wideband stair-shaped dielectric resonator antennas, in IET Microwaves," *Antennas & Propagation*, vol. 1, no. 2, pp. 299–305, April 2007.

[11] M. Lapierre, Y. M. M. Antar, A. Ittipiboon, and A. Petosa, "Ultra wideband monopole/dielectric resonator antenna," *IEEE Microwave and Wireless Components Letters*, vol. 15, no. 1, pp. 7–9, 2005.

[12] A. Petosa, *ielectric Resonator Antenna Handbook (Artech House Antennas and Propagation Library)*, Artech House, Norwood, MA, USA, 2007.

[13] P. Gupta, D. Guha, and C. Kumar, "Dielectric resonator working as feed as well as antenna: new concept for dual-mode dual-band improved design," *IEEE Transactions on Antennas and Propagation*, vol. 64, no. 4, pp. 1497–1502, 2016.

[14] S. Fakhte, H. Oraizi, and L. Matekovits, "High gain rectangular dielectric resonator antenna using uniaxial material at fundamental mode," *IEEE Transactions on Antennas and Propagation*, vol. 65, no. 1, pp. 342–347, 2017.